

## Photogrammetry-based reverse engineering method for aircraft airfoils prediction

Mohammed A. Ba Zuhair\*

*Technische Universität Hamburg (TUHH), Institute für Lufttransportsysteme,  
Blohmstr. 20, 21079 Hamburg, Germany*

*(Received May 30, 2021, Revised September 9, 2021, Accepted November 30, 2021)*

**Abstract.** Airframe internal and external specifications are the product of intensive intellectual efforts and technological breakthroughs distinguishing each aircraft manufacturer. Therefore, geometrical information characterizing aircraft primary aerodynamic surfaces remain classified. When attempting to model real aircraft, many members of the aeronautical community depend on their personal expertise and generic design principles to bypass the confidentiality obstacles and sketch real aircraft airfoils, which therefore vary for the same aircraft due to the different designers' initial assumptions. This paper presents a photogrammetric shape prediction method for deriving geometrical properties of real aircraft airframe by utilizing their publicly accessible static and dynamic visual content. The method is based on extracting the visually distinguishable curves at the fairing regions between aerodynamic surfaces and fuselage. Two case studies on B-29 and B-737 are presented showing how to approximate the sectional coordinates of their wing inboard airfoils and proving the good agreement between the geometrical and aerodynamic properties of the replicated airfoils to their original versions. Therefore, the paper provides a systematic reverse engineering approach that will enhance aircraft conceptual design and flight performance optimization studies.

**Keywords:** aerodynamics; aircraft design; airfoil aerodynamics; conceptual design; numerical simulation; other relevant topic

---

### 1. Introduction

Recent progress in computational equipment and capabilities has encouraged many individuals, previously not included in the official aerospace community such as freelance engineers, researchers, hobbyists and students to get involved in the innovative aeronautical research. Today, interest in designing and simulating manned/unmanned aerial vehicles and scaled-down real aircraft models is growing. When starting a real aircraft designing or re-engineering project, the first obstacle facing the independent designers worldwide is how to acquire well-validated geometrical data describing the selected commercial/military aircraft airframe or its parts such as fuselage, wing and etc. (Sun *et al.* 2020). This difficulty is attributed to the fierce competitiveness requisites in the aviation market necessitating complete confidentiality of similar information. As a result, freelance or amateur designers depend on their own expertise and professional skills aided by generic aircraft design and performance principles to generate the required geometries to be

---

\*Corresponding author, Ph.D. Student, E-mail: mohammed-ba@yandex.ru

used as baselines for iterative and multivariate performance improvement studies as conducted by Sun *et al.* (2020) and Orlita *et al.* (2017). However, vast differences in personal expertise, skills and flawed assumptions often result in producing geometrically variant versions of the same product, especially for wings, blades and fairings, therefore causing subsequent inconsistencies and discrepancies in their simulated aerodynamics and dynamics when performing cross-validation studies, e.g. see B738 in (Sun *et al.* 2020, SUAVE 2018).

One of the systematic shape re-production methods for aeronautical applications to overcome the above-described problem is Reverse Engineering (RE). The primary workflow of RE usually starts with scanning the actual body to virtually replicate its surface points using photogrammetric devices (Olejnik *et al.* 2018, Wang *et al.* 2020). The photogrammetric method is also applied for general and/or partial airframe geometry deformation analysis with respect to crashworthiness, icing, wing bending and structural studies as reported by Justin (2016), Aicardi *et al.* (2020) and Demoulin *et al.* (2020). Next, various digital processing phases may be considered to export specific file formats of the obtained points data. In the final stage, this data becomes represented in the form of surface and solid bodies using some points interpolation code commonly known as Computer-Aided Design and Manufacturing (CAD/CAM) software (Gómez *et al.* 2017, Huband 1997, Optical Measuring Techniques, 2008, Potabatti 2019, Xiong *et al.* 2011). Today, most of the popular CAD/CAM tools offer add-ins for RE (Buonamici *et al.* 2018). Current advances in optical scanning devices accompanied with powerful CAD/CAM software enable accurate digital representation of all aircraft parts and components, or even the whole airframe, once these bodies are physically available. Therefore, such geometries exhibit the closest aerodynamic characteristics to the original model when simulated for the same boundary conditions. However, operations such as acquiring either an aircraft internal or external part or the entire airframe, subsequent storing and optical scanning are neither possible nor affordable for most independent designers from the public. Again, the latter remain deprived of any real aircraft geometrical data unless published by the manufacturer, which often happens after the aircraft is long out of service. To make the situation worse, almost all critical performance data are also kept secret. This also applies to the aerodynamic characteristics, therefore hindering any rigorous validation of the RE-based predicted geometries. In result, when attempting to independently investigate or optimize an actual aircraft geometric or performance, the researcher is left blind of any validation possibilities, which ingrains a low credibility on all results he can attain.

To solve both problems of unknown geometrical and experimental data, aeronautical research agencies such as NASA, JAXA, and DLR have recently agreed to provide limited publicly-shared solid and meshed aircraft models appended to fully-described experimental conditions and results as shown in the AIAA CFD High Lift Prediction Workshops (2020). Although this definitely builds a valuable database for external and independent aeronautical scholars to verify their Computational Fluid Dynamics (CFD) codes and basic high-lift aerodynamics analyses as seen in Ashton and Skaperdas (2019), one should also indicate the limitedness of such information usability. For example, all published geometries are intended for high-lift wind tunnel experiments with stripped off tail surfaces. This devaluates their application for full takeoff and landing aerodynamic simulations, where wheels, rudders, and spoilers may play a vital role in the flow dynamics. Furthermore, wing, fuselage and high-lift system configurations of these common research models (RCMs) feature generic airframe configurations, i.e. they do not represent an actual aircraft shape or high-lift devices which undervalues RCMs CFD results utilization for realistic takeoff and landing simulations.

To avoid uninformed aircraft shaping, another data-driven RE approach is commonly adopted

by using firstly basic blueprints and aircraft information provided in the flight manuals and secondly general conceptual aircraft design principles to estimate the main flight performance parameters in cruise, takeoff, and landing (De Grave 2017, Werner-Spatz *et al.* 2009). These methods work best for steady flight modes and yield rapid low-fidelity predictions for regulated performance parameters such as liftoff, touchdown, and cruise for which performance margins and constraints are typically known. However, this RE method does not provide helpful representative geometrical data for detailed external aerodynamics analyses and optimizations.

In this paper, we propose a new shape recognition method of arbitrary streamlined body geometrical information through the implementation of image-processing techniques on the two-dimensional aircraft images of available for public access. In particular, this paper focuses on real aircraft wing shaping as being the most complex and relevant, yet the same workflow applies to vertical and horizontal stabilizers design. Furthermore, the presented method may be also functionally extended and integrated with CAD/CAM codes to replicate many real-world objects using proper representative digital images.

## 2. Method description

Current practice of designing an arbitrary aircraft full configuration typically begins with searching its reliable images depicting a number of schematic three-dimensional projections of the aircraft body. Such inputs usually happen to be the manufacturer blueprints, which qualify for serving as a guiding background reference for sketching and surfaces generation. These blueprints are often found in the aircraft characteristics and airport planning manuals. They are of high-resolution and detail major external geometrical characteristics such as aircraft layout, relative sizes of airframe parts, besides demonstrating generic representations of fuselage, wing and tailplanes dimensions. Thus, open access blueprints offer a valuable starting point for obtaining accurate frontal, side and planform geometrical definitions. Here, this advantage is being tapped as well. However, some important features including wing, vertical and horizontal stabilizers sectional details are kept confidential. This is common in scientific reports of military and commercial aircraft, which besides concealing geometrical information also contain uninformative aerodynamic graphs, i.e. effaced numeric data. This makes them of little use for further cross - analysis and -validation purposes by third parties (Sun *et al.* 2020). To overcome the wing sections classification problem, we propose the employment of real aircraft images visualizing some of the required wing and tailplanes inboard and intermediary cross-sectional edges. The approach is based on the following processing rules:

- All imported-aircraft imagery should expose at least one aerodynamic surface fairing edge with another component. It is also prerequisite to single out only images of sufficient resolution and contrast, wherein airframe parts fairing and edges can be visually distinguished.
- Only side-view images, where small aircraft body rotation/inclination is observed, are accepted. Such effects result from aircraft body rotation or/and askew observer shooting/filming angles. Filtering out image samples based on minimum obliqueness effects helps to minimize corrupted edge extractions associated with the virtual squeezing and flattening of the distinctive wing and tailplane edges as aircraft body rotates, which is illustratively demonstrated in Fig. 1. Thus, it is reasonable to establish a limit of +15...-30° observer-aircraft angle for a good perception of the potential leading-edge and camber flexures.
- Scaled-down replicates of a preceding airfoil surface curve can be used for generating curve

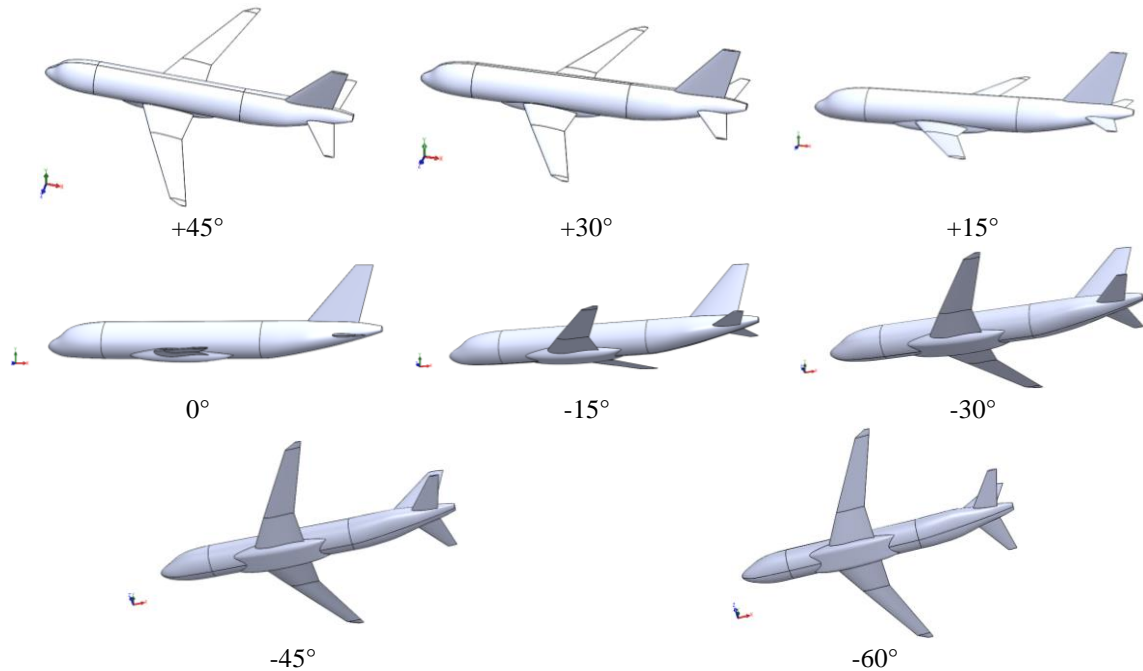


Fig. 1 Typical aircraft body rotation scenarios encountered in the moment of photographing/filming

coordinates of an undefined posterior sectional shape. In most cases, this rule helps in approximating the upper segment of mid-wing supercritical airfoils aligned with pylons. In addition, sketching and lofting of airframe parts with a spanwisely invariable airfoil becomes easier.

### 2.1 Processing steps

Photogrammetric airfoil shaping workflow described in this section is partially automated at this initial phase of the research. In general, the process of acquiring sectional geometrical data of a specific aircraft begins with searching and importing of numerous side-view images that satisfy the aforementioned stringent illumination, contrast and picturing/filming angle requirements. There are two key sources of such inputs: digital images and video recordings. Despite of their abundance, freely accessible images of many aircraft are practically incompatible with the above-stated filtering requirements because they were not taken for airframe photogrammetric recognition and reconstruction purposes. Therefore, it is recommended to input self-captured images for any aircraft under consideration. Unfortunately, this task cannot be always accomplished. During the course of digital images mining attempts, it was concluded that for modern aircraft, high-resolution airshow and aircraft promotion visual contents provide high-quality diverse graphical samples. In particular, such videos can enable extracting tens of appropriate static frames for a specific aircraft type. Note that for accurate and reliable outputs, only real in-flight/on-ground aircraft snapshots should be used. Thus, animations, simulator three-dimensional models and other computer renderings should be excluded since they are mostly defected and based on their own designer approximations.

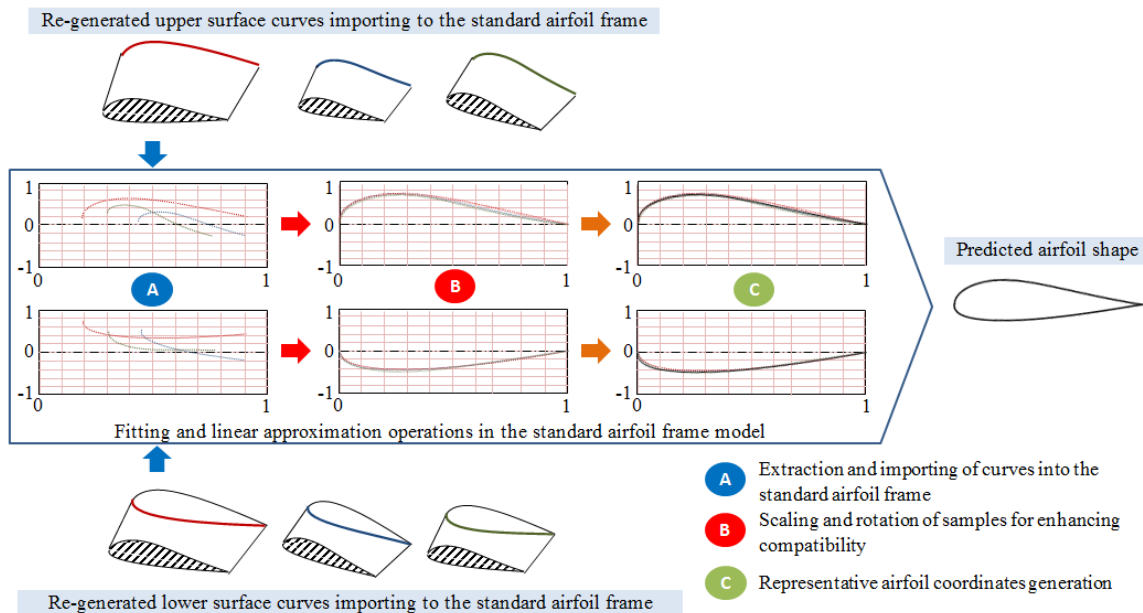


Fig. 2 Schematic workflow representation of the main steps to predict an arbitrary airfoil shape

Next, the accumulated images are sorted in the database in accordance with the visible aircraft part and its view (upper or lower). To be more specific, the first group consists of images representing airframe parts of interest, e.g. the wing, the vertical or horizontal stabilizer, while the second group contains the corresponding part visible side, i.e. lower or upper. In result, a single aircraft part, for instance the wing, becomes represented by a two-column matrix. When collecting graphical samples for wing airfoils, aircraft images in cruise configuration should be prioritized. This preference is driven by the observed clean wing configuration which facilitates the extraction of wing inboard and mid-sections airfoils without geometrical deformations caused by the deployed high-lift and flow spoiling devices or landing gear releasing hatches in other flight modes. These difficulties are irrelevant to horizontal and vertical stabilizers as they hold constant shapes during almost the entire flight envelop. At the end of this phase, a group of carefully imported images (samples) become usable for extracting airfoil coordinates.

Airfoil representation is performed using the reliable B-spline interpolation method (He *et al.* 2019, Pérez-Arribas *et al.* 2016). For B-splines generation, samples are fixed as a static background while B-splines are generated on an upper floating layer to enable direct visual verification. Note that wing/fuselage fairing edges are the most distinguishable, thereby proposing the easiest spot for inboard section airfoil recognition and extraction as illustratively demonstrated in Fig. 3. Components attached to the wing surface may also create geometrically distinctive edges, e.g. flap track fairings and engine pylons on the lower wing surface. Sometimes, images of this type can be successfully employed for approximating the aerodynamic mean chord airfoil and its neighboring ones, see W1" and W2". Because of the lack of such visually trackable edges on the upper wing surface, the third rule is applied to facilitate generating complete airfoil curves for these particular airfoils, see W1' and W2' in Fig. 3. Unfortunately, outboard airfoils of most aerodynamic surfaces, i.e. wing and tailplanes, are difficult to obtain using the current method due to the absence of any visually detectable edges or cuts. For tailplanes, this problem is overcome by

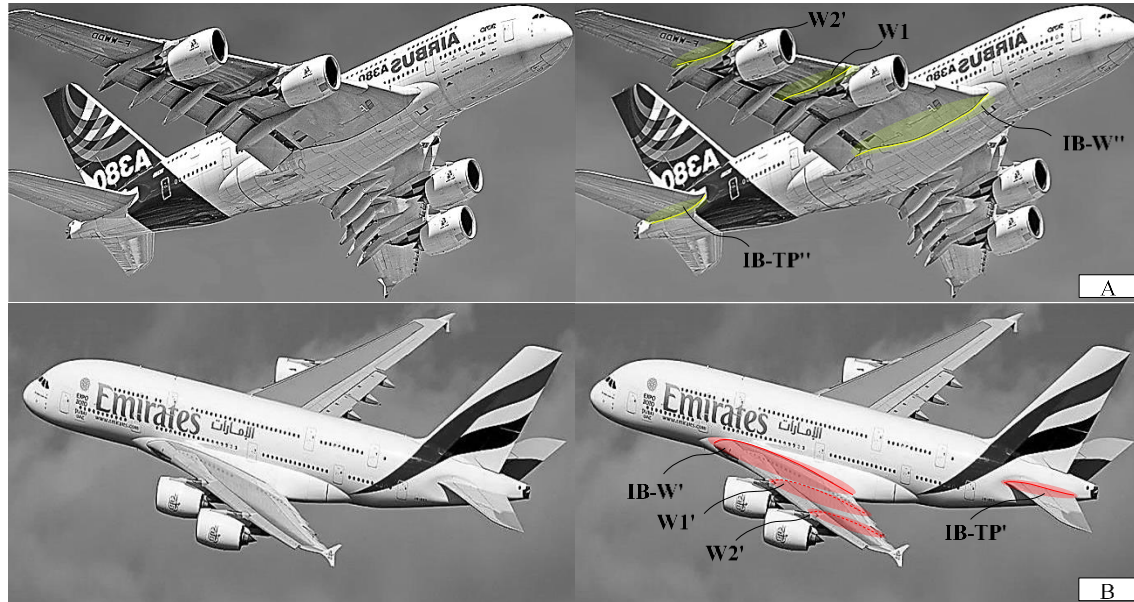


Fig. 3 Airfoil sections extracted directly or indirectly from a A380 digital images overlapped by extracted airfoil curves, where IB-TP is the inboard tailplane airfoil, IB-W is the inboard wing airfoil, W1, W2, mid-wing airfoils curves. Note that the upper commas denote the extracted airfoil surfaces location, where ' stands for the upper surface segment and '' for the lower one. The dotted airfoil upper surface curves W1' and W2' in Fig. 2(B) indicate the indirect sketching approach used for their creation by extending IB-W' to W1' and W2' locations and proportionally scaling-down each curve. Original images used under CC BY 2.0 license from (Green 2010, Visser 2013)

evoking the relevant design principles which state that symmetrical and identical airfoils should be used for both vertical and horizontal stabilizer cross-sections (Sadraey 2012). Thus, the inboard airfoil can be propagated throughout these part spans. However, a knowledge-based approximation method for the wing outboard section is still sought for until now.

After generating all airfoil curves from the samples in phase Fig. 2(A), these curves must be processed to enhance dimensional compatibility in Fig. 2(B). For this purpose, every re-generated upper or lower curve becomes projected on a graphical interface supported by an image digitalizer, where angle of attack (AoA) and chord line length abbreviated as “c” are fixed, see Fig. 2. Thus, AoA is assumed zero and curve coordinates are normalized in accordance with the common airfoil shaping theory, i.e.  $x_i/100$  and  $y_i/100$ . This step is necessary because the imported raw curves from phase (A) often have slightly different lengths or inclinations due to the different image-capturing perspectives. To ensure dimensional compatibility, isotropic re-scaling and curve rotation are allowed, i.e. no additional curve points are introduced. However, leading and trailing edges points sometimes need to be extended or trimmed to match the corresponding boundary points reference centerline. Distortions in the airfoil leading and trailing edge regions stem from the fact that some original images do not reveal exact initial and last aerodynamic surface leading and trailing points due to shadow effects or slats and flaps deployment. This deformity is transferred to the replicated curves as well. To resolve it, some stretching or point displacements is necessary to achieve exact superposition with the centerline edges. In other cases, slight shadows may blur sectional edges, which may reflect on the predicted chamber line curvature and maximum airfoil thickness value.

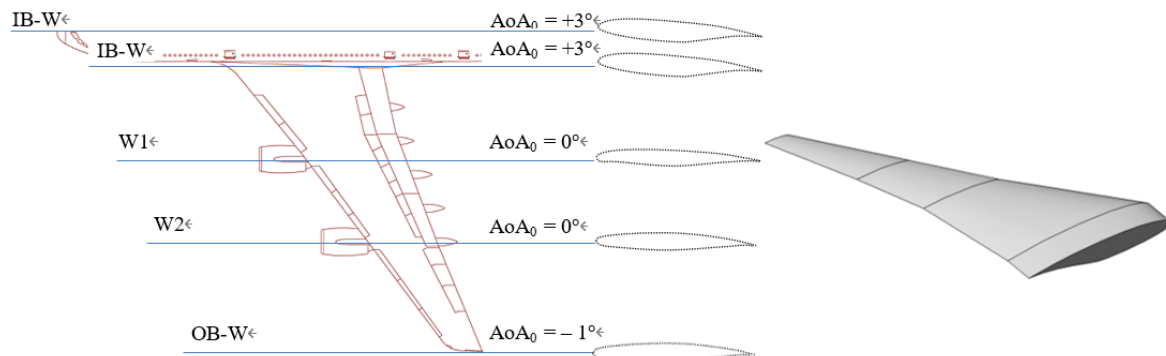


Fig. 4 Adopted three-dimensional wing model generation using predicted airfoil sections

However, it is noteworthy to emphasize the advantage of applying aircraft-observer angle smallness filtering rule above, which minimizes such potential unacceptable edge distortions.

To generate  $x_i$  and  $y_i$  coordinates of the predicted airfoil in Fig.2 (C), the image digitalization code coupled with the standard airfoil frame is used to compute the mean of y-axis points according to  $\bar{y}_i = \sum_{i=1}^N (N^{-1}y_i)$ , where  $N$  is the curves amount. As a result, a single predicted airfoil is produced, i.e. the black curve in Fig. 2. The described process must be followed to generate all sectional airfoils on the wing, tailplanes.

When proceeding to build CAD models, e.g. for the wing, the predicted airfoils are sketched on side-planes matching locations of airframe parts they are extracted from. For this purpose, manufacturer blueprints are valuable, see Fig. 4. For wing inboard section (IB-W), it is assumed that the encompassed within the fuselage wing section shape replicates the visible one on the wing-belly fairing side, thus it can be extruded from it. Another approach may consider lofting in accordance with the wing taper up to the fuselage centerline. In addition, due to the currently difficult extraction of the wing outboard (OB-W) section airfoil it may be considered as an offset of the preceding one, i.e. W2 in Fig. 3. Meanwhile, IB-W and OB-W sections should adhere to their design angles of attack (AoA0) requirements typically defined as  $+3^\circ$  for IB-W and  $-1^\circ$  for OB-W as shown in Fig. 4. Although tailplanes are not generated here since they are less complex, the same procedures are applicable. Note that obtaining images for the vertical stabilizer may be a harder task when scanning open access relevant images. However, the established practice recommends using promotional and airshow videos of the manufacturer or credible third parties especially for new aircraft generations.

### 3. Geometric and aerodynamic validations

The establishment of a conclusive judgment on this method accuracy and feasibility is further examined using two validation approaches. The first validates the appropriateness of the implemented classification and geometric features recognition to generate geometrically valid airfoil shapes for reliable knowledge-based real aircraft aerodynamic analysis and optimization studies. In Fig. 5, we compare exact inboard section airfoils of the B-29 and B-737 from Airfoils database (2021) and their predicted versions. For executing this mission, a set of nine B-29 and four B-737 (-100) images was collected and processed. The smaller quantity of B-737 samples is

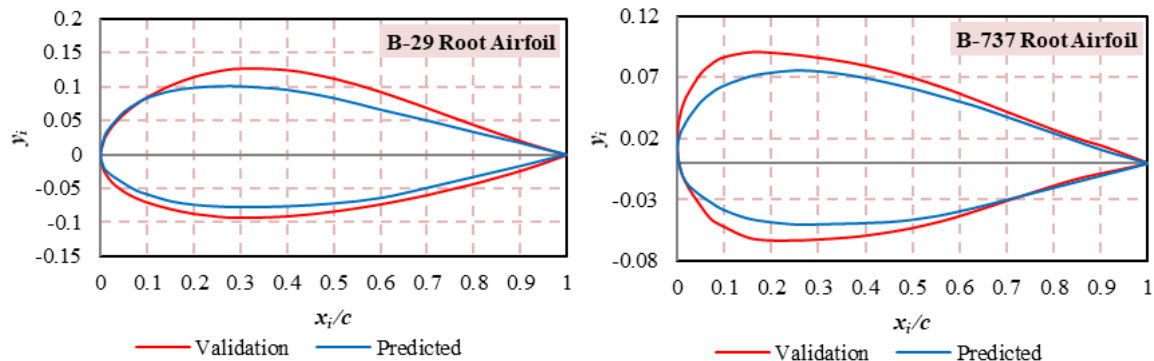


Fig. 5 Surface curve coordinates of the predicted and validation B-29 and B-737 inboard wing section airfoils

caused by its early version poor and valid accessible digitalized photographic archives in the open access galleries. The predicted inboard airfoils from both aircraft are shown in Fig. 5, where good convergence is observed near the leading and trailing edges. However, a growing divergence is noticed as airfoil thickens indicating that both predicted airfoil coordinates are blemished by an underestimated maximum thickness and camber scale and position values. This discrepancy is a consequence of the following three factors: a) shadow effects blurring wing edges especially at lower surface; b) clockwise/counter clockwise aircraft body rotations at the moment of most graphical recordings, consequently hindering precise detection of wing edge curves, as previously shown in Fig. 1; c) far-view complications in some images in which wing leading edge details are visually difficult to determine. Additionally, temporarily modified leading and trailing edges curvatures due to the deflected high-lift devices during climb, approach, and near-ground flight can mislead initial points and leading curvature estimation as well. These problems could be solved by a supervised photographing process, e.g. when aircraft is on the ground. Furthermore, observations reveal that new and popular aircraft generations enjoy abundant accessible image archives of high quality and reliability. This seems valuable for any future aircraft airfoils replication plan. In general, it can be concluded that predicted airfoils show acceptable geometrical agreement with the validating samples. To further support this claim, a second investigation is conducted to assess the scale of the geometrical variance impact on the resultant flowfield properties and aerodynamics.

For computational aerodynamics, we apply XFOIL 6.99 code written for developing and optimizing two-dimensional airfoil representations in subsonic flow regimes (Drela 2000). All airfoils are formatted according to Selig  $x_i$  and  $y_i$  arrangements and simulated in an inviscid flow mode at Reynolds number ( $Re$ ) of  $5.0 \cdot 10^6$  using 280 surface panels and 200 iterations. The selected  $Re$  value falls in the typical range appropriate for simulating takeoff and landing phases using wind tunnels and computational fluid dynamics (CFD).

As known, airfoil camber and thickness directly affect overall pressure field and transitional properties around the airfoil. In a previous statement, it was reported that estimated airfoil coordinates differ from the original versions in two aspects: undervalued maximum thickness by 70-80% and shifted maximum camber position by  $\sim \pm 12\%$ . When tracking the resultant effects, a first look is given into the evolving pressure regions around the top and bottom airfoil surfaces using the associated dimensionless representation, i.e. pressure coefficient ( $C_p$ ) shown in Fig. 6(a)

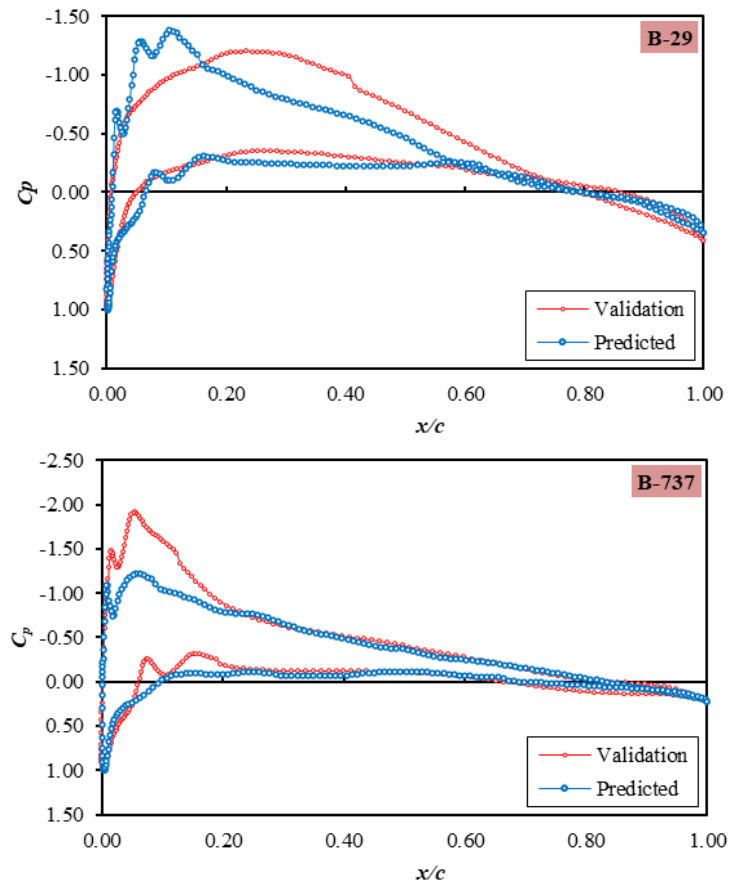


Fig. 6 Distributions of pressure coefficient around the predicted and validation airfoils

and 6(b) for the inboard wing design angle  $+3^\circ$ . Here, a clear view is provided for both cases, where a higher pressure zone covering the upper surface mid-section of the predicted B-29 airfoil is observed in comparison to the validating case. In the case of B-737, better agreement is established, which is meanwhile defected by a stronger and smoother pressure gradient that dominates the maximum thickness region up to  $0.22c$  on both airfoil sides.

Besides, the observed local pressure re-distributions indicate modified boundary layer evolution and transition behavior. In Fig. 7(a) and (b), we demonstrate boundary layer transitional history as all airfoils move towards the stalling limits, where it is shown that initial transition point locations are altered due to the geometrical dissimilarities. Here, we see that both initial transition points of the predicted B-29 airfoil exhibit a 20% displacement in contrast to the B-737 case. Moreover, higher sensitivity of both predicted airfoils to the flowfield vector gradient, i.e. AoA change, majorly on the top surface is noticed as well. The latter translates into a stronger tendency to rapid thickening of the boundary layer, which causes earlier and larger turbulence propagation as the AoA increases.

After assessing flowfield modifications, it is worthy to highlight the resulting global aerodynamics effects. In Fig. 8, we compute lift and drag coefficients, i.e.  $C_L$  and  $C_D$ , respectively, at selected AoA starting from zero degrees up to the characteristic stall value matching

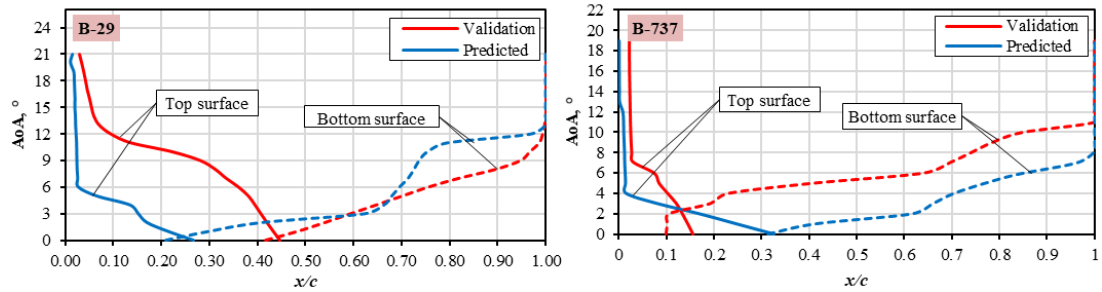


Fig. 7 Transition point displacement recordings as AoA increases for both the predicted and validation airfoils

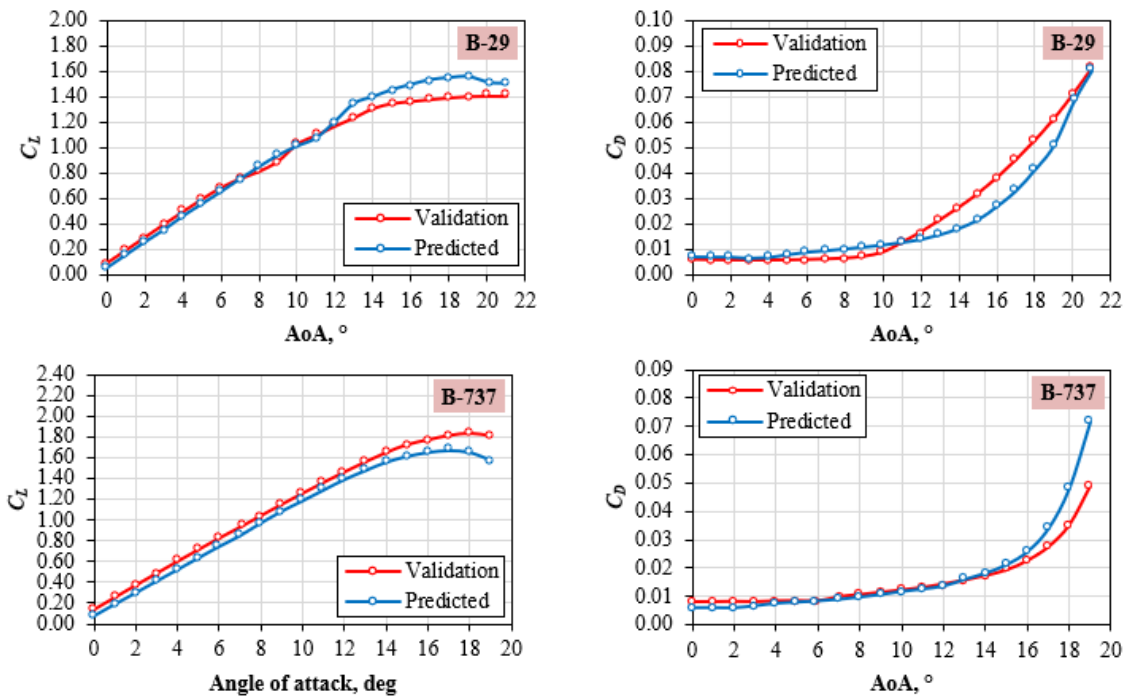


Fig. 8 lift and drag coefficients of the predicted and validation airfoils in the range of operational

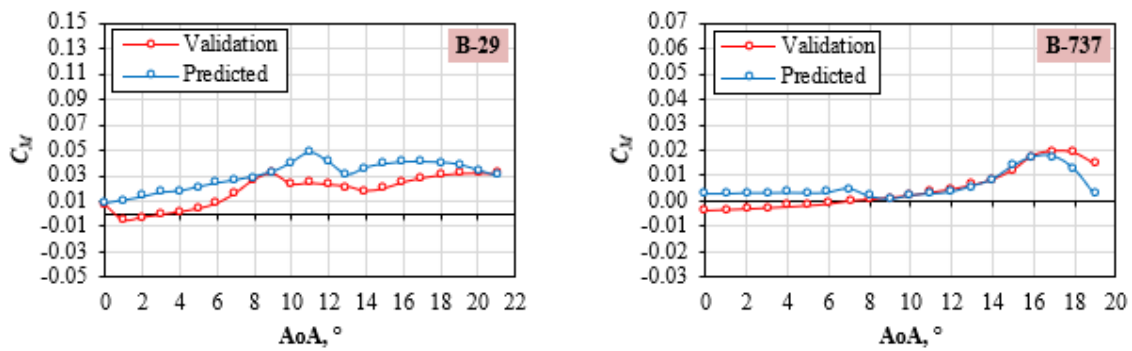


Fig. 9 Pitching moment coefficient of the predicted and validation airfoils in the range of operational AoA

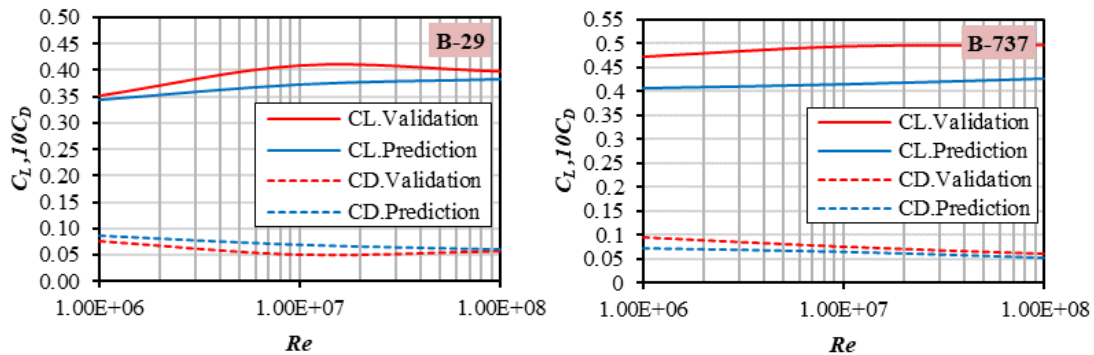


Fig. 10 Lift and drag coefficients variations versus increasing  $Re$  specifying the predicted and validation airfoils

approximately  $21^\circ$  and  $19^\circ$  for B-29 and B-737, respectively. These plots show good alignment with the validating data along the lift slope AoA up to  $14^\circ$ , after which aerodynamic forces begin to suffer divergence or instabilities. Fundamentally, the latter is constituted by the above-described separation effects. These phenomena also influence airfoil rotational dynamics expressed in terms of the pitching moment ( $C_M$ ) as demonstrated in Fig. 9. Here, it is shown that nose-up moment generally converges as expected up to the stalling range of AoA.

#### 4. Discussion

Previous aerodynamic analysis of the predicted airfoils indicates that the imperfect geometrical agreement with the original shapes induces limited aerodynamic performance penalties, especially in the case of B-737. This tendency is observed at moderate  $Re$  scales, but Fig. 10 shows that investigating  $C_L$  and  $C_D$  variations at lower and higher turbulence ranges still confirms the established overall consistency. Due to the applied software limitations, transonic flow simulations achieved during cruise flight were not conducted, although wave drag contributions caused by flow compressibility effects are not expected to drive new divergence trends.

Overall geometrical and aerodynamic validations show that the proposed method can be reliable for many engineering applications. The method offers a systematic data-driven approach for predicting most aerodynamic surfaces geometries of conventional aircraft configurations whose fairing edges are visual and distinguishable. Thus, this framework enables realistic flight performance modelling and optimization of many operating and retired commercial and military aircraft. In this regard, it is important to report the major encountered applicability limitations, which are found to be associated with highly-smoothed or blended wing and tail parts fairings. Fairings blending is common on most combat aircraft, e.g. stealth fighters and airplanes, as an inevitable geometrical requirement for decreasing side body radar cross-sections. The same applies to current and future military and commercial aircraft concepts derived from flying wing configurations, in particular, flying wings and blended-wing bodies. Nevertheless, it should be hinted that even these aircraft can expose some of their looked-for geometric features in certain airframe images characteristic by favorable shadow effects. In addition, a well-instructed photographing or filming campaign and further smart processing techniques can also facilitate such a task.

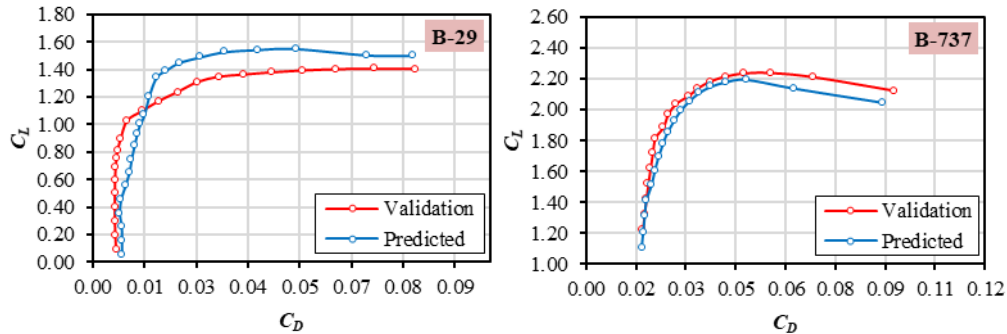


Fig. 11 Drag polar graphs resulting from a trailing edge spoiler (B-29) and leading and trailing flaps (B-737) for the predicted and validation airfoils

The utmost importance of an accurate airfoil shape prediction is the consequent ability to realistically model cruise modes, where aerodynamic performance depends on the clean wing and tailplane geometrical properties. However, when modelling transitional flight modes such as takeoff, climb, approach, and landing, it is noticed that airfoil shape modifications by the deployed high-lift devices or spoilers reduce the potential impact of predicted airfoils inaccuracies as long as flap, slat, and spoilers settings and geometrical specifications are correctly defined for the aircraft under study. To illustrate this, Fig. 11 demonstrates two possible airfoil configurations, where in the B-29 case a trailing edge spoiler located at  $0.8c$  and deflected by  $+30^\circ$  (upwards) is simulated. For the second case, i.e. B-737, typical takeoff high-lift devices settings are introduced using a leading edge flap located at  $0.15c$  and a similar one at  $0.8c$  both set at  $-15^\circ$  and  $-25^\circ$  (downwards), respectively. For both scenarios, AoA starts from  $0^\circ$  and increases by  $+1^\circ$ . As seen, a better agreement is observed when more high-lift devices are attached, see B-737. This is attributed to the fact that these devices, when deflected, largely alter pressure distributions around the airfoil surface and contribute the most of its aerodynamics. Therefore, when simulating landing rolls, where flaps, slats, and spoilers, are all deployed at maximum degrees, ranging between  $\pm 0^\circ \dots 60^\circ$ , this RE method results enjoy higher tolerance to the possible inherent shapes discrepancies and produce closer predictions to the original sections.

## 5. Conclusions

In this paper, we attempted to present a systematic aircraft aerodynamic surface re-shaping method that utilizes publically accessible digital image albums for this purpose. This method is valuable for aircraft body RE applications and tackles the problem of confidential airfoil wing and tail parts geometries definition. The method consists of three steps: image accumulation and classification, visual geometric features extraction, and final predicted airfoils approximation to a single linearly-approximated shape. Two validation studies were conducted to highlight method uncertainties and show its good geometrical and aerodynamic predictions. The paper has also outlined major current limitations effecting both applicability and accuracy. This leads to concluding that successful application and integration of the current method are expected to enhance shape and performance predictability of aircraft design tools and boost their realistic aerodynamic shape optimization capabilities. In addition, the proposed aircraft body RE promises to leverage aircraft big data and provide generalized predictive models for disclosing aircraft

proprietary aerodynamic characteristics with minimized human-designer involvement and assumptions.

Most of the data acquisition and geometric features extraction activities, and further analyses models, conducted in the framework of this study were neither automated nor compiled with each other. This significantly decelerated the process of analyzing large sets of imagery content and limits the method scalability to human-constrained capabilities. Therefore, an extended RE model utilizing machine learning techniques will expand this nascent RE method version and enable creating large libraries of various airfoils of most operating and retired aircraft types. To achieve this goal, a big and verified images database (various aircraft types, parts and views) must be beforehand generated for purposes of training and testing. This process requires careful data collection, thus it is laborious and time-consuming. For airfoil shaping automatization, advanced image-processing techniques can be applied for curve parameterization using appropriate color segmentation and morphological operations coupled with efficient point datasets interpolation methods all synthesized and represented in a single user-friendly toolset.

## References

- AIAA CFD High Lift Prediction Workshops (2020), 4th AIAA CFD High Lift Prediction Workshop (HLPW-4); AIAA & NASA, USA, <https://hiliftpw.larc.nasa.gov/Workshop4/geometries.html>.
- Aicardi, I., Lingua, A., Mazzara, L., Musci, M.A. and Rizzo, G. (2020), "Ice detection on airplane wings using a photogrammetric point cloud: A simulation", *Proceedings of the International Archives of Photogrammetry, Remote Sensing and Spatial Information Sciences*, **43**, 183-189. <https://doi.org/10.5194/isprs-archives-xliiii-b2-2020-183-2020>.
- Ashton, N. and Skaperdas, V. (2019), "Verification and validation of OpenFOAM for high-lift aircraft flows", *J. Aircr.*, **56**(4), 1641-1657. <https://arc.aiaa.org/doi/abs/10.2514/1.C034918>.
- UIUC Applied Aerodynamics Group (2021a), B29 Root Airfoil; University of Illinois at Urbana-Champaign, Illinois, U.S.A. <https://m-selig.ae.illinois.edu/ads/coord/b29root.dat>.
- UIUC Applied Aerodynamics Group (2021b), B737a Airfoil; University of Illinois at Urbana-Champaign, Illinois, U.S.A. <https://m-selig.ae.illinois.edu/ads/coord/b737a.dat>.
- SUAVE (2018), Boeing 737 Using AVL; Stanford Aerospace Design Lab, California, U.S.A. <https://suave.stanford.edu/tutorials/avl.html>.
- Buonamici, F., Carfagni, M., Furferi, R., Governi, L., Lapini, A. and Volpe, Y. (2018), "Reverse engineering modeling methods and tools: a survey", *Comput. Aided Design.*, **15**(3), 443-464. <https://doi.org/10.1080/16864360.2017.1397894>.
- De Grave, E. (2017), "Reverse engineering of passenger jets—classified design parameters", M.Sc. Thesis, Hamburg University of Applied Sciences, Hamburg, Germany.
- Demoulin, Q., Lefebvre-Albaret, F., Basarab, A., Kouamé, D. and Tourneret, J. Y. (2020), "A new flexible photogrammetry instrumentation for estimating wing deformation in airbus", *Proceedings of the ETTC2020: European Test and Telemetry Conference*, Online, June.
- Drela, M. (2000), XFOIL Subsonic Airfoil Development System; Massachusetts Institute of Technology, Cambridge, Massachusetts, USA. <https://web.mit.edu/drela/Public/web/xfoil/>.
- Gómez, A., Olmos, V., Racero, J., Ríos, J., Arista, R. and Mas, F. (2017), "Development based on reverse engineering to manufacture aircraft custom-made parts", *Int. J. Mechatron. Manuf. Syst.*, **10**(1), 40-58.
- Green, R. (2013), A6-EDY A380 Emirates 31 Jan 2013 JFK; Flickr, Bedford, U.K. <https://www.flickr.com/photos/miqspix/4843636798/>.
- He, X., Li, J., Mader, C.A., Yildirim, A. and Martins, J.R. (2019), "Robust aerodynamic shape optimization – from a circle to an airfoil", *Aerosp. Sci. Technol.*, **87**, 48-61. <https://doi.org/10.1016/j.ast.2019.01.051>.
- Huband, J.M. (1997), "Reverse engineering of aircraft wing data using a partial differential equation surface

- model”, Ph.D. Dissertation, Old Dominion University, Virginia, USA.
- Littell, J.D. (2016), *Experimental Photogrammetric Techniques Used on Five Full-Scale Aircraft Crash Tests*, National Aeronautics and Space Administration (NASA), Langley Research Center, Virginia, U.S.A.
- Olejnik, A., Kiszowski, L., Dziubiński, A. (2018), “Aerodynamic modeling process using reverse engineering and computational fluid dynamics”, *Proceedings of the Earth and Space 2018: Engineering for Extreme Environments*, Virginia, U.S.A., April.
- Optical Measuring Techniques (2008), Application Example: Reverse Engineering Aerospace: Digitizing of a full-scale Falcon 20 “Zero-g” jet aircraft; GOM mbH, Braunschweig, Germany.  
[https://www.gom.com/fileadmin/user\\_upload/industries/falcon\\_EN.pdf](https://www.gom.com/fileadmin/user_upload/industries/falcon_EN.pdf).
- Orlita, M. and Vos, R. (2017), “Cruise performance optimization of the airbus A320 through flap morphing”, *Proceedings of the 17th AIAA Aviation Technology, Integration, and Operations Conference*, Denver, U.S.A., June.
- Pérez-Arribas, F., Castañeda-Sabadell, I. (2016), “Automatic modelling of airfoil data points”, *Aerosp. Sci. Technol.*, **55**, 449-457. <https://doi.org/10.1016/j.ast.2016.06.016>.
- Potabatti, N. S. (2019), “Photogrammetry for 3D reconstruction in solidworks and its applications in industry”, M.Sc. Thesis, Purdue University Graduate School, Indiana, U.S.A.
- Sadraey, M. H. (2012), *Aircraft Design: A Systems Engineering Approach*, John Wiley & Sons, Chichester, U.K.
- Sun, J., Hoekstra, J.M. and Ellerbroek, J. (2020), “Estimating aircraft drag polar using open flight surveillance data and a stochastic total energy model”, *Transport. Res. C Emer.*, **114**, 391-404.  
<https://doi.org/10.1016/j.trc.2020.01.026>.
- Visser, M. (2010), Überflug in Airbus-Werkslackierung; Flicker, California, U.S.A.  
[https://de.wikipedia.org/wiki/Airbus\\_A380#/media/Datei:Airbus\\_A380\\_overfly\\_crop.jpg](https://de.wikipedia.org/wiki/Airbus_A380#/media/Datei:Airbus_A380_overfly_crop.jpg).
- Wang, Y.M., Yu, S.Y., Ren, S., Cheng, S. and Liu, J.Z. (2020), “Close-range industrial photogrammetry and application: review and outlook”, *Proceedings of the Optics Ultra Precision Manufacturing and Testing Conference*, Beijing, China, November.
- Werner-Spatz, C., Heinze, W. and Horst, P. (2009), “Improved representation of high-lift devices for a multidisciplinary conceptual aircraft design process”, *J. Aircr.*, **46**(6), 1984-1994.  
<https://doi.org/10.2514/1.42845>.
- Xiong, J., Tang, S. and Guo, J. (2011), “Approach of aircraft configuration with complex free-form surface design based on reverse engineering”, *Proceedings of the 2011th International Conference on Electronic & Mechanical Engineering and Information Technology*, Harbin, China, March.